Sensitivity Analysis of Switched Reluctance Motor for Potential Application in Electric Vehicles Considering Weight Factor

Karunakaran Vijayalakshmi† and **Kandadai Nagaratnam Srinivas**, Non-members

ABSTRACT

The switched reluctance motor (SRM), an environmentally friendly machine, is suitable for application in electric vehicles (EV) in recent days. This paper presents an SRM sensitivity analysis focussing on weight of the materials used for stator and rotor for use in electric vehicle application. Two SRM structures are considered, namely normal stator tooth and tapered stator tooth. Thirteen materials widely used in the SRM are considered for these two structures to perform the proposed sensitivity analysis. The major outputs of torque, speed, power, iron loss, efficiency, copper loss, and power factor are gathered through finite element analysis (FEA) simulation. Each of the 13 materials are examined for normal tooth and tapered tooth geometrical structures. The results are discussed, focusing on the fitness of the considered SRM structures for EV application. As weight-sensitive vehicles, the materials used in EVs are compared against the respective motor weights obtained through analysis to recommend the lightest motor for production.

Keywords: Switched Reluctance Motor, SRM, Electric Vehicle, EV, Sensitivity Analysis

1. INTRODUCTION

Due to its numerous advantages, such as low cost, absence of magnets, high-temperature operation, robustness, and high-speed operation, the SRM is attaining wider application, especially in electric vehicles. A literature survey on the use of the SRM in EV applications is presented in this section, from which the scope of the research is derived. The analyses conducted in [1, 2] demonstrated that the torque of the tapered structure in the stator is better than the straight tooth structure. The main factors considered in the design of EVs and HEC applications are discussed in [3], namely output power capability, torque-speed characteristics, torque ripple analysis, DC link voltage variations, weight of the motor, and total cost. Genetic algorithm analysis was carried in [4] to find the optimum torque.

In the design of parameters, the authors considered stator diameter and rotor tooth width (both root and tip). Dimensions such as the taper angle of the stator poles, rotor, and stator pole arc angles were examined to optimize the parameters of the SRM and provide reduced torque ripple, improved torque, torque density, and loss for applications involving EVs in [5]. The genetic algorithm was used for optimization.

The optimized asymmetric bridge converter was proposed in [6] to provide higher torque at low speed when compared to the existing model. Optimization of the SRM involved five parameters: radius of the rotor slot, stator slot, rotor tooth, angular width of the rotor and stator teeth, and slope of the teeth. The authors also analyzed the turn-on and turn-off angles of the asymmetric bridge converter. The 6/4 pole SRM was designed using a high-temperature superconducting material to improve the current carrying capability, with tapering poles to optimize the magnetic circuit in [7]. It has been proven that torque density can be improved by 29% compared to the conventional machine due to the new tapered pole design. A new SRM design was adopted by [8] for comparison with the existing one to improve the torque and motor energy conversion capacity [8]. The authors also discussed the static and dynamic characteristic of the SRM with 6/4 and 8/6 geometries. In [9], the SRM is compared with an induction motor and BLDC and proven to be the best in certain circumstances. The turn-on and turn-off angles, current set level, and optimum control parameters of the SRM were also discussed. In [10], a 102 kW machine was designed with improved efficiency and reduced torque ripple for electric vehicle propulsion.

Based on this survey, it can be observed that a sensitivity analysis on the tapering stator at its yoke root has not been carried out. Furthermore, such a dimensional design is expected to offer less iron loss when the area of the back-core width is reduced. Thus, an SRM structure with tapered stator poles at its yoke root is considered for sensitivity analysis in this current research work, focusing on EV applications.

2. TORQUE AND DIMENSIONS

The parametric requirements for machines used in EV applications are high torque density, high starting torque,

Manuscript received on June 22, 2021; revised on October 20, 2021; accepted on December 01, 2021. This paper was recommended by Associate Editor Kaan Kerdchuen.

The authors are with the Department of Electrical and Electronics Engineering, Faculty of Engineering and Technology, SRM Institute of Science and Technology, Ramapuram Campus, Chennai, India.

†Corresponding author: vijik.rk@gmail.com

Digital Object Identifier: 10.37936/ecti-eec.2022202.246904

high power density, operational capability in harsh environments, peak overload capability, low acoustic noise, a constant power operating range of 3–4 times the base speed, low torque ripple, and low cost. Therefore, machines selected for EV application should satisfy the above conditions.

The SRM is suitable for application in EV since it satisfies the key parameters:

1. It offers high power density and robustness [11].
2. It has shown equivalent performance to the interior permanent magnet synchronous motor (IPMSM) used in the 2009 Toyota Prius and demonstrated a better response than the IPMSM at higher speeds [12].

The SRM is a doubly salient singly excited machine with windings only in the stator and none on the rotor. The torque in the SRM depends on the current flowing through the phases and its change in inductance with respect to the rotor position. Eqs. (1)–(3) are the general equations for the SRM.

The torque equation for the SRM is

$$T = \frac{1}{2} i^2 \frac{dL}{d\theta}. \tag{1}$$

The inductance equation is written as

$$L = \frac{N\Phi}{I} \tag{2}$$

$$\text{Flux} = \frac{MMF}{S} = \frac{NI}{S} \tag{3}$$

where Φ = flux (weber); N = no. of turns (T); I = current (A); S = reluctance (AT/weber).

Since the number of turns and the current through a given coil are fixed, the only parameter making the flux vary is variable reluctance (changing the rotor position) in the SRM. In the SRM, when the stator coil is energized, the rotor will try to align itself with the minimum reluctance position. As the rotor tries to align itself with the energized stator pole, the reluctance of the circuit varies. The flux linkage then varies according to the inductance. Therefore, the derivative of the current with respect to time is not zero, although the current is constant. The calculations given below for torque, power, and speed are obtained from the simulation results.

For normal tooth structure, the power at 1000 rpm is

$$P_m = T \cdot \omega = 1.4 \cdot (2\pi \times (1000/60)) = 146.533 \text{ W}.$$

For tapered tooth structure, the power at 1000 rpm is

$$P_m = T \cdot \omega = 1.154 \cdot (2\pi \times (1000/60)) = 120.78 \text{ W}$$

and outer dimensions

$$D_{si} = D_r + 2 \cdot g$$
$$D_{so} = (1.5 - 1.8) D_{si}$$

where D_{si} = inner diameter of stator in mm, g = air gap in mm, D_r = rotor diameter in mm and D_{so} = outside stator diameter in mm.

In this paper, the design is as follows according to the expression, $D_{so} = 70$ mm and $D_r = 34.2$ mm.

Stator inside diameter

$$D_{si} = D_r + 2 \cdot g = 34.2 + 2(0.4) = 35 \text{ mm}.$$

Stator outside diameter

$$D_{so} = (1.5 - 1.8) D_{si} = 1.8 \times 35 = 63 \text{ mm}.$$

The foregoing calculations represent the designed dimensions of the SRM under study for EV applications. Two different configurations are proposed for performance analysis: a normal stator tooth and a tapered stator tooth, both with the same outside diameter, gap length, stack height, number of slots per pole, and outside diameter of the stator and rotor.

Materials play a vital role in the performance of the SRM as well as its overall weight, as far as the machine's application for EV is concerned. To ascertain the two parameters for discussion, sensitivity analysis is carried out on the finite element (FE) platform, considering the 13 different materials suitable for EV manufacture. Thus, 13 materials are examined for two different SRM structures to predict performance and weight.

Furthermore, these analyses are extended for operating speeds ranging from 1000 to 10000 rpm.

The SRM data sheets for the normal stator tooth and tapered tooth structures are presented in the following section. The analysis is carried out on two different structures with the same outside dimensions for the stator and rotor. In this study, 13 stator and rotor materials are selected to observe the performance of the machine in terms of weight, torque, and efficiency since these parameters are important in EV application. The previously mentioned design calculations are fine-tuned and finally fixed as follows. These values are used for simulation and analysis.

2.1 Dimensions of stator and rotor in SRM (normal tooth)

Stator;

- Number of slots = 6,
- Outside diameter = 70 mm,
- Inside Diameter = 39 mm,
- Tooth width = 8 mm.

Rotor;

- Number of poles = 4,
- Outside diameter = 34.2 mm,
- Diameter of shaft = 10 mm.

2.2 Dimensions of stator and rotor in SRM (tapered tooth)

Stator;

- Number of slots = 6,

- Outside diameter = 70 mm,
- Inside Diameter = 35 mm,
- Tooth width = 6.9 mm.

Rotor;

- Number of poles = 4,
- Outside diameter = 34.2 mm,
- Diameter of shaft = 11.4 mm.

3. SRM FOR EV APPLICATION

The ratings of an electric rickshaw are 1200 W, 60/72 V, 83%, while the speed ranges from 4800/6100 rpm (referred from Changzhou Sunlight Motor Co., Ltd). In this paper, the power rating for both structures is 1 kW. The rating of voltage and power in an electric auto-rickshaw application can be compared with that of the SRM in this paper. Accordingly, the speed ranges selected are 4800 and 6100 rpm. In this paper, the results are analyzed at various speeds ranging from 1000 to 10000 rpm to find the maximum values for torque and efficiency. The results show that the tapered stator tooth in this paper exhibits about 85% efficiency in the higher speed range. The efficiency of the normal stator tooth structure is slightly less than for the tapered tooth structure at a higher speed.

3.1 Proposed geometric modifications

Since the tapering of the stator pole at its yoke root can exhibit reduced iron loss, this process is proposed here, although, to date, it has not been performed in existing research.

The material used for the stator and rotor core in the SRM generally consists of M19 steel, which has a core loss of approximately 2.93 W/kg (it varies according to the thickness of the material). The following materials are used in this paper: 50A230, 50A250, 50A270, 50A290, 50A310, 50A350, 50A400, 50A470, 50A600, 50A700, 50A800, 50A1000, and 50A1300, which have a thickness of 0.5 mm and a core loss of 2.30 W/kg, 2.70 W/kg, 2.90 W/kg, etc., coming under the category of hot rolled sheets. Hot rolled steel has better mechanical properties than cold rolled steel, as well as improved tensile strength and reduced residual stress. These materials show less core loss and high permeability and are widely used in small transformers and rotating machines. Table 1 presents the data sheet of other core materials for reference. In this paper, materials 50A230 and 50A290 are considered since they provide improved performance in terms of efficiency and torque compared to all the other materials used.

4. STATIC FINITE ELEMENT ANALYSIS

4.1 Dimensions of the SRM

The proposed SRM structures with a normal stator pole and tapered stator pole are shown in Figs. 1(a) and (b), respectively. Figs. 1(c) and (d) show the dimensions of the stator and rotor for normal and tapered tooth structures. These dimensions are used in the simulation of the SRM in JMAG Designer software. The mesh analysis is shown in Figs. 1(e) and (f) for normal and tapered tooth structures.

***Table 1**: Datasheet of other core materials.*

Grade	Thickness inch (mm)	Max Core Loss at 1.5 T			
		Watts per kilogram		Watts per pound	
		50 Hz	60 Hz	50 Hz	60 Hz
M-15	0.014	2.53	3.20	1.15	1.45
M-19	(0.36)	2.75	3.48	1.25	1.58
M-22		2.93	3.70	1.33	1.68
M-27		3.13	3.97	1.42	1.80
M-36		3.31	4.19	1.50	1.90
M-15	0.085	2.93	3.70	1.33	1.68
M-19	(0.47)	3.03	3.83	1.37	1.74
M-22		3.22	4.08	1.46	1.85
M-27		3.31	4.19	1.50	1.90
M-36		3.57	4.52	1.62	2.05
M-43		4.01	5.07	1.82	2.30
M-45		5.31	6.72	2.41	3.05
M-47		6.96	8.82	3.16	4.00
M-19	0.025	3.62	4.58	1.64	2.08
M-22	(0.64)	3.80	4.80	1.72	2.18
M-27		3.92	4.96	1.78	2.25
M-36		4.18	5.29	1.90	2.40
M-43		4.70	5.95	2.13	2.70
M-45		6.27	7.93	2.84	3.60
M-47		8.53	10.80	3.87	4.90

4.2 Pre-processing, processing, and post-processing

In this study, the SRM model is imported from JMAG Express into JMAG Designer. The two-dimensional model selected comprises the specification and subdivision of machine geometry. The parts are named according to the structure and boundary conditions assigned to the model in the JMAG Designer software.

The model for numerical analysis has a stator, rotor, stator field coils, and a shaft. Each component is modeled by specifying its physical properties, including the stator/rotor material, coil resistance, number of turns, sequence of coils, etc.

4.2.1 Pre-processing

In JMAG Designer, once the model has been created, the toolbox will be available at the right side of the window where the material templates for assignment and analysis are placed. To set the conditions, it is necessary to click on the material tool from the toolbox and select the material to be applied to the stator, rotor, and shaft. The real machine is thus simulated.

1. The periodic boundary conditions for rotation are to specify the periodic boundary for the model. The following conditions are set in the periodic boundary: (i) periodicity-anti periodic and (ii) periodic angle 180.
2. When the periodic angle option is selected, an arrow appears on the screen. The face with the periodic

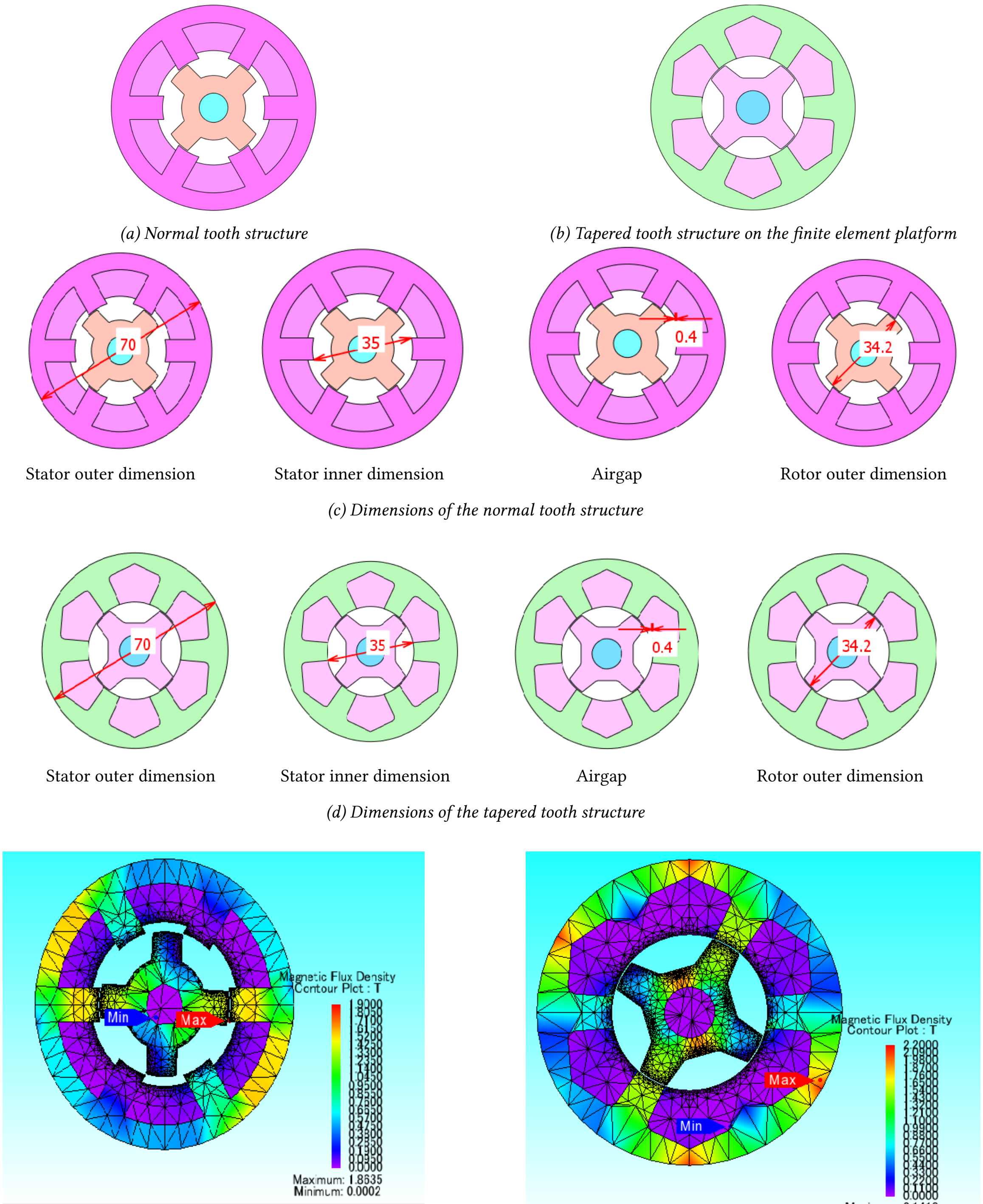

(a) Normal tooth structure

(b) Tapered tooth structure on the finite element platform

Stator outer dimension Stator inner dimension Airgap Rotor outer dimension

(c) Dimensions of the normal tooth structure

Stator outer dimension Stator inner dimension Airgap Rotor outer dimension

(d) Dimensions of the tapered tooth structure

(e) Mesh model of the normal tooth structure

(f) Mesh model of the tapered tooth structure

Fig. 1*: Model of the SRM.*

boundary condition and the face with the same geometry (the one that will be the second periodic boundary face) must exist in front of the arrow. If the arrow points in the opposite direction to that intended, the rotation axis must be reversed.

3. FEM coil:
   - This specifies the linkage of the FEM coil in the model to the FEM coil component in the circuit.
   - The coils are U, V, and W phase coils. The value of the resistance and number of coil turns will be specified in the FEM coil block.
   - The pull-down menu shows the FEM coil component on an external circuit. From there, a related component is chosen. The resistance of the coil uses an electric circuit in conjunction with the FEM coil. It does not function on its own. One FEM coil

component can be supported by a single FEM coil condition. A different FEM coil condition is set if the associated FEM coil component is different.

4. Motion rotation specifies the rotational motion of parts. The motion condition can be used as a reference when setting the force/torque condition applied for the nodal force and surface force. The motion condition is set before using the force/torque condition as referenced. During the formation of a slide mesh (translation motion), the area where a motion condition is set extends to include part of the air region. The area where a force condition is set also extends upon the selection of a motion region, thereby increasing the calculation accuracy.
5. The torque condition is used to calculate the torque acting on the specified parts of a model. The force condition is used to calculate the electromagnetic force acting on the specified parts of a model. The entire calculation region of the electromagnetic force/torque circumstances is employed to obtain an electromagnetic force distribution. Each node receives its own set of results.
6. The slide condition is specified when the model moves by motion. The slide condition is set for the boundary face between the mover and stator. In JMAG, this boundary face is referred to as the "slide face". Motion is accounted for during analysis by changing the mover side mesh one step at a time. The mesh region has been specified.

4.2.2 Processing

The processing is carried out in JMAG Designer software. To determine the magnetic field distribution inside the motor, the following assumptions are made. (i) The magnetic material of the stator and rotor cores is isotropic. (ii) The outer limits of the motor are treated as zero vector potential since the magnetic field in that area is negligible.

The partial differential equation for calculating the magnetic vector potential vector A is written as:

$$\frac{\partial}{\partial x}\left(\frac{\partial \overline{A}}{\partial x}\right)+\frac{\partial}{\partial y}\left(\frac{\partial \overline{A}}{\partial y}\right)=-\mu J \tag{4}$$

In Eq. (4), the current flowing through the coil is a known parameter, and the magnetic vector potential is the unknown parameter. The value of current density J can be identified by the current value, and hence the magnetic vector potential can be calculated. It is too complex to calculate the vector potential manually, and therefore FEA is performed to attain $\overline{A}$. Using Eq. (4) with the appropriate boundary condition, the value of the magnetic vector potential can be calculated. Due to the nonlinear characteristics, numerical methods are chosen instead of an analytical solution. The solution is obtained as in Eq. (5),

$$F=\int\left(\int_0^B HdB - J\cdot\overline{A}\right)dR \tag{5}$$

where R is termed as the problem region of integration.

The entire problem region is subdivided into finite elements that coincide with the boundary of each material. Once the problem has been identified, the solver will not require user interaction to obtain the results.

With the magnetic vector potential value in hand, the magnetic flux density and other derivable quantities for electromagnetic analysis are calculated, as explained in the following section. These calculations form the post-processing stage.

4.2.3 Post-processing

At this stage, the mathematical solution for the potential values is processed to obtain the results. The other electromagnetic values are derived from the magnetic vector potential using Eqs. (6)–(9).

$$B=\Delta\times\overline{A} \qquad \text{(magnetic flux density value)} \tag{6}$$

$$\phi=\frac{B}{A} \qquad \text{(flux)} \tag{7}$$

$$\psi=N\varphi \qquad \text{(flux linkage)} \tag{8}$$

$$L=N\frac{\varphi}{i} \qquad \text{(inductance)} \tag{9}$$

4.3 Results and discussion

Figs. 2(a) and (b) present the simulation output plot for the magnetic flux density of normal tooth and tapered tooth structures. From this plot, the value obtained is 1.5 T, which is approximately equal to the material flux density. In Fig. 3, the stator and rotor pole variation in reluctance is shown according to its aligned, slightly aligned, and unaligned positions. The torque in the SRM is directly proportional to the square of the current, which is similar to the series motor and will have a high starting level. This is a key point for two-wheelers or four-wheelers in EV application. Fig. 4 shows that the flux density is at maximum in the aligned position and lower in the unaligned position. Fig. 3 indicates the maximum and minimum flux distributions in the aligned and unaligned positions. The reluctance element plays an important role in the SRM. Table 2 presents the results for the simulation of normal tooth and tapered tooth structures at 1000 rpm for reference.

4.4 Factors to be considered for electric vehicle application (weight, torque, and efficiency analysis)

Normal tooth structure, for EV application, the weight of the machine is one of the important factors to consider. Therefore, the normal tooth structure weighs less when materials 50A230, 50A250, 50A270, and 50A290 are used in comparison to the others. The results reveal that in the

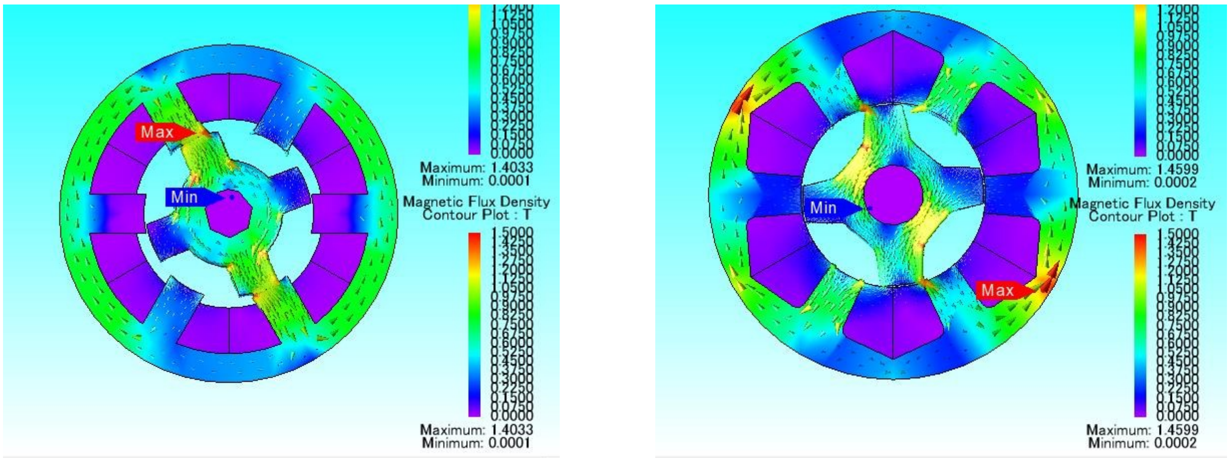

(a) (b)

Fig. 2: *Nominal flux density distribution: (a) normal tooth structure and (b) tapered tooth structure. The excited stator poles show the designed flux density of 1.5 T in both cases. The results shown are for material 50A230.*

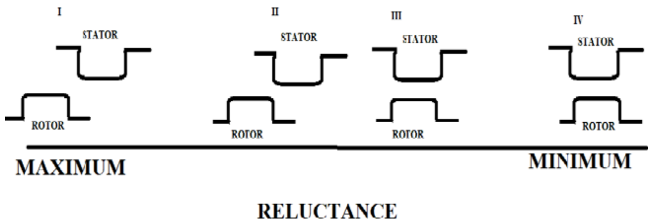

Fig. 3: *Diagram of the switched reluctance motor.*

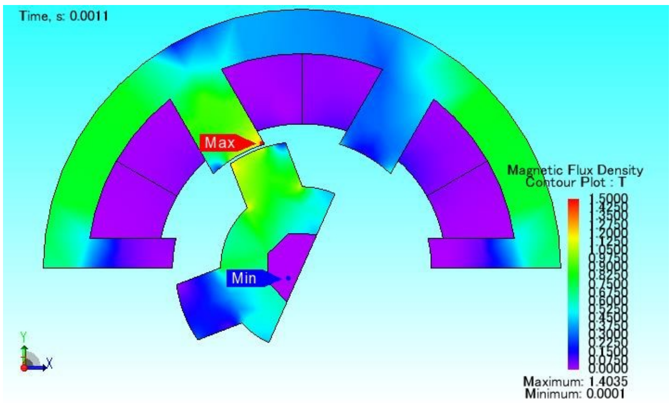

Fig. 4: *Structure of the normal tooth SRM. Maximum flux density is attained when the stator and rotor are in the aligned position.*

normal tooth, material 50A290 shows improved torque compared to the others (50A230, 50A250, and 50A270). With respect to efficiency, 50A230 shows high efficiency at 9000 rpm compared to the others.

Tapered tooth structure, the machine in the tapered tooth also weighs less when materials 50A230, 50A250, 50A270, and 50A290 are used in comparison to the others. The results reveal that 50A290 exhibits the maximum torque compared to the other materials (50A230, 50A250, and 50A270.) Material 50A230 shows maximum efficiency at 8000 rpm compared to 50A250, 50A270, and 50A290.

Therefore, from the simulation results, it can be observed that material 50A230 exhibits the maximum efficiency in comparison to all the other materials used in both normal and tapered tooth structures (50A230, 50A250, and 50A270). Material 50A290 shows high torque in comparison to all the other materials analyzed.

Table 3 presents a comparison between different materials and their weights. It can be observed that the machine weighs less when using 50A230, 50A250, 50A270, and 50A290 materials for both structures in comparison to other materials.

Table 4 presents the torque, efficiency, and power val-

***Table 2**: Parameters of the SRM with normal tooth and tapered tooth structure at 1000 rpm.*

Parameters	SRM (normal tooth)	SRM (tapered tooth)
Type	50A230	50A230
Coil category	copper	copper
Weight	2.14	2.186
DC voltage	60 V	45 V
Voltage application start angle (degree)	5	5
Application width (mechanical angle) (degree)	30	30
Maximum current	45 A	45 A
Revolution speed (rpm)	1000	1000
Torque	1.4 Nm	1.154 Nm
Efficiency	50.32%	45.93%
Power	146.6 W	120.8 W
Power factor	0.2394	0.2392
Copper loss	139.6 W	139.4 W
Iron loss	5.182 W	2.832 W

***Table 3**: Comparison between different materials and their weights (kg). The bold values in kg indicate that the weight remains the same for the respective materials.*

Materials/ structure	Normal tooth (kg)	Tapered tooth (kg)
50A230	**2.14**	**2.186**
50A250	**2.14**	**2.186**
50A270	**2.14**	**2.186**
50A290	**2.14**	**2.186**
50A310	2.149	2.195
50A350	2.149	2.195
50A400	2.149	2.195
50A470	2.159	2.203
50A600	2.168	2.212
50A700	2.177	2.221
50A800	2.177	2.221
50A1000	2.186	2.229
50A1300	2.186	2.229

***Table 4**: Torque and efficiency values at different speeds. The bold values indicate the maximum levels for torque and efficiency in the normal tooth and tapered tooth structure.*

Speed/structure	Normal Tooth Torque in Nm (50A290)	Efficiency in % (50A230)	Tapered Tooth Torque in Nm (50A290)	Efficiency in % (50A230)
1000	1.40851	50.3234	1.1581	45.9321
2000	1.47061	66.5259	1.222	63.2867
3000	1.5152	73.9491	1.2694	71.9712
4000	1.54255	77.9877	1.3033	76.9904
5000	**1.55893**	80.3312	1.3265	80.1105
6000	1.44899	81.4955	**1.3427**	82.1518
7000	1.06582	82.6107	1.2510	83.641
8000	0.798792	**82.7989**	1.0954	84.7691
9000	0.627999	82.6853	0.8559	**85.0235**
10000	0.510218	82.0007	0.6908	84.8491

ues at different speeds, ranging from 1000 to 10000 rpm. As can be observed, the maximum value for the torque is achieved for the normal tooth structure, while the tapered tooth structure exhibits high efficiency.

4.5 Validation of Theoretical and Simulation Results

4.5.1 Normal tooth structure

The torque equation can be represented as follows:

$$T = \frac{P}{(2\pi N/60)} \text{ (Nm)}$$
$$T = \frac{816.256}{(2\pi 5000/60)} = 1.5597 \text{ Nm (Theoretical)}$$

where power (P) is referred from the simulation results given in Table 4. The torque at 5000 rpm is 1.55893 Nm (practical) (as shown in Table 4).

The efficiency of the motor can be calculated as follows

$$\text{Efficiency } (\eta) = \frac{\text{Output power}}{\text{Input power}} \times 100$$

output power = 146.6 W. Therefore,

$$\begin{aligned} \text{input power} &= \text{output power} + \text{losses} \\ &= 146.6 + 139.6 + 5.182 = 291.382 \\ \text{Efficiency} &= \frac{146.6}{291.382} \times 100 \\ &= 50.311\% \text{ (Theoretical).} \end{aligned}$$

The efficiency at 1000 rpm is 50.32% (practical) (as shown in Table 4).

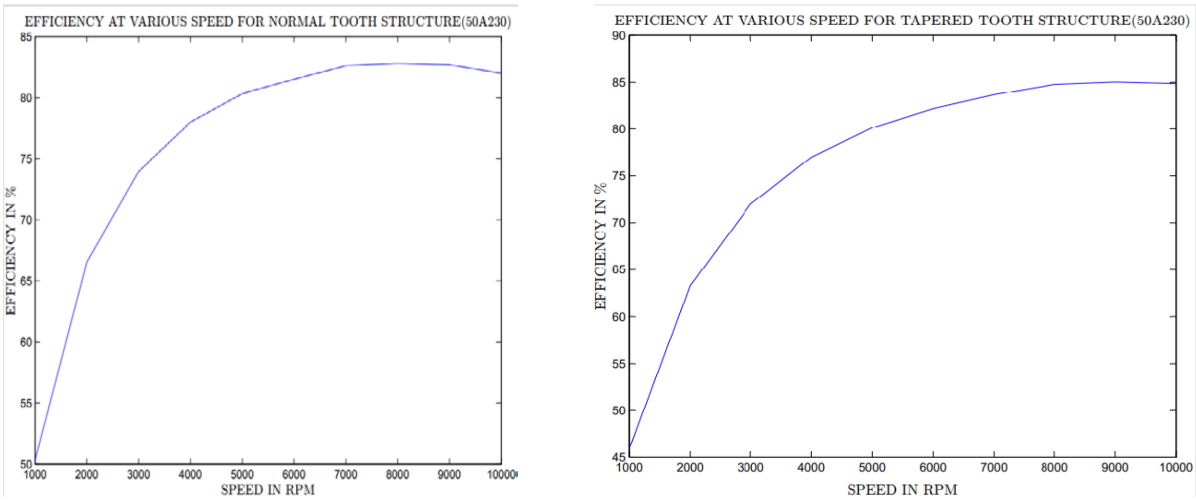

(a) *(b)*

Fig. 5*: Efficiency plot of the various speeds for (a) the normal tooth structure and (b) the tapered tooth structure.*

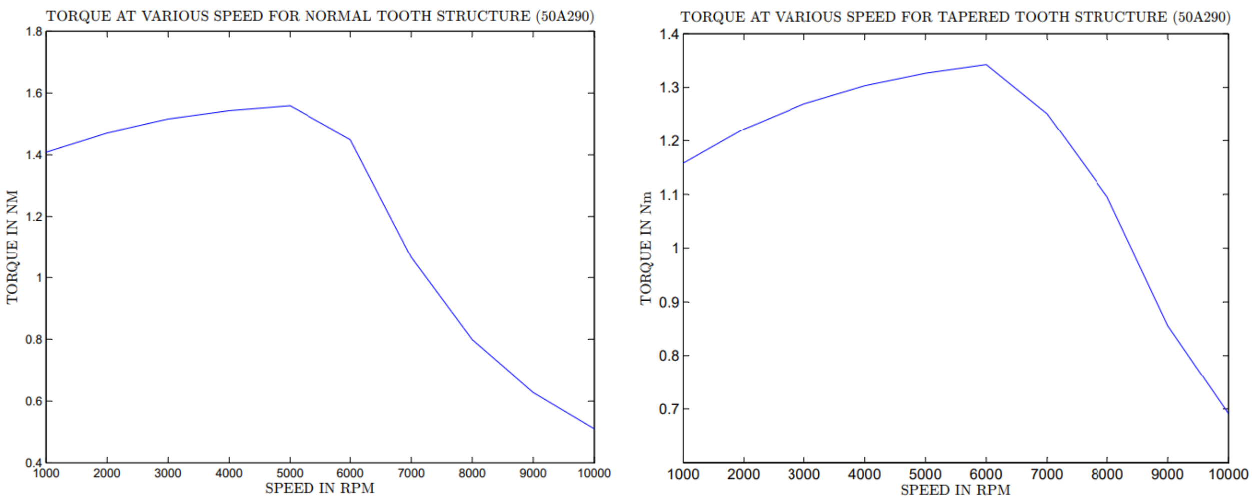

(a) *(b)*

Fig. 6*: Torque at various speeds for (a) the normal tooth structure and (b) the tapered tooth structure. The tapered tooth demonstrates better torque up to 8000 rpm, whereas the machine with the normal tooth exhibits good torque up to 6500 rpm.*

4.5.2 Tapered tooth structure

$$T = \frac{843.672}{(2\pi 6000/60)} = 1.3434 \ \text{Nm (Theoretical)}$$

The torque at 6000 rpm is 1.34275 Nm (practical) (as shown in Table 4).

The efficiency of the motor can be as follows

$$\begin{aligned} \text{output power} &= 120.8\,\text{W} \\ \text{input power} &= \text{output power} + \text{losses} \\ &= 120.8 + 139.4 + 2.832 = 263.032 \\ \text{Efficiency} &= \frac{120.8}{263.032} \times 100 \\ &= 45.62\% \ \text{(Theoretical)}. \end{aligned}$$

The efficiency at 1000 rpm is 45.93% (practical) (as shown in Table 4).

4.6 Discussions

Figs. 5 and 6 show the torque and efficiency curve for normal and tapered tooth structures. The results indicate that maximum efficiency is achieved at the higher speed range. According to the simulation results, it is clear that the efficiency is high for the tapered tooth structure compared to the normal tooth for material 50A230. At the same time, the simulation results also indicate that the maximum torque is obtained for normal tooth structure compared to the tapered tooth for the same material 50A290. Therefore, according to the simulation results, it can be observed that material 50A230 shows improved efficiency in the tapered tooth structure while 50A290 shows the maximum torque for the normal tooth structure.The theoretical and simulation results are discussed in Section 4.5. The density of 50A230 material is 7600 kg/m^3 and the density of 50A1300 is 7850 kg/m^3.

The Electromagnetic FEA simulation provides the variation of flux density, B, in wb/m^2, for the rotor positions of 0° to 360°. It is observed that the value of B reaches a maximum of 2.8 wb/m^2, under excited stator pole in the case of material 50A1300, whereas the same value reaches 3 wb/m^2 in the case of material 50A230. This is an evidence to note that 50A230 has a lesser weight over 50A1300 because B is inversely proportional to weight.

In [13], a wide literature review for the reduction of torque ripple, noise, and vibration in switched reluctance to make it as a suitable candidate in electric vehicle application is discussed.

5. CONCLUSION

Due to its various advantages, the SRM is suitable for electric buses and other and EV applications. In this paper, the weight, torque, and efficiency of the machine are analyzed since these are the most important factors to consider in EV application. As can be observed from the simulated results, both the normal and tapered tooth structures exhibit less weight when materials 50A230, 50A250, 50A270, and 50A290 are used in comparison to the remaining materials.

When comparing the normal and tapered tooth structures, 50A290 shows a greater improvement in torque with less weight. Therefore, if the application requires high torque, 5A290 should be selected as the core material.

In a comparison between the normal and tapered tooth structures, 50A230 shows higher efficiency than all the other materials, with less weight. Therefore, if the application requires high efficiency, 50A230 should be selected as the core material.

Since torque, weight, and efficiency are important parameters in EV applications, the comparison of the simulated results is based on these two factors.

REFERENCES

[1] L. Sitsha and M. Kamper, "Some design aspects of tapered and straight stator pole 6:4 switched reluctance machine," in *IEEE 5th African Conference*, Cape Town, South Africa, 1999, pp. 683–686.

[2] C. Neagoe, A. Foggia, and R. Krishnan, "Impact of pole tapering on the electromagnetic torque of the switched reluctance motor," in *1997 IEEE International Electric Machines and Drives Conference Record*, Milwaukee, WI, USA, 1997, pp. WA1/2.1–WA1/2.3.

[3] G. Pellegrino, A. Vagati, B. Boazzo, and P. Guglielmi, "Comparison of induction and PM synchronous motor drives for EV application including design examples," *IEEE Transactions on Industry Applications*, vol. 48, no. 6, pp. 2322–2332, Nov. 2012.

[4] U. Sholahuddin, A. Purwadi, and Y. Haroen, "Structural optimizations of a 12/8 switched reluctance motor using a genetic algorithm," *International Journal of Sustainable Transportation Technology*, vol. 1, no. 1, pp. 30–34, Apr. 2018.

[5] M. Ćosović, S. Smaka, I. Salihbegović, and Š. Mašić, "Design optimization of 8/14 switched reluctance machine for electric vehicle," in *2012 XXth International Conference on Electrical Machines*, Marseille, France, 2012, pp. 2654–2659.

[6] T. Ishikawa, Y. Hashimoto, and N. Kurita, "Optimum design of a switched reluctance motor fed by asymmetric bridge converter using experimental design method," *IEEE Transactions on Magnetics*, vol. 50, no. 2, pp. 781–784, Feb. 2014.

[7] K. Zhang, X. Huang, J. Zhang, L. Wu, Y. Fang, and Q. Lu, "Design and analysis of a switched reluctance motor with superconducting windings and tapering poles," *IEEE Transactions on Applied Superconductivity*, vol. 26, no. 7, Oct. 2016, Art. no. 5208204.

[8] S. R. Mousavi-Aghdam, M. R. Feyzi, N. Bianchi, and M. Morandin, "Design and analysis of a novel high-torque stator-segmented SRM," *IEEE Transactions on Industrial Electronics*, vol. 63, no. 3, pp. 1458–1466, Mar. 2016.

[9] K. Rahman, B. Fahimi, G. Suresh, A. Rajarathnam, and M. Ehsani, "Advantages of switched reluctance motor applications to EV and HEV: design and control issues," *IEEE Transactions on Industry Applications*, vol. 36, no. 1, pp. 111–121, Jan. 2000.

[10] A. Omekanda, "A new technique for multidimensional performance optimization of switched reluctance motors for vehicle propulsion," *IEEE Transactions on Industry Applications*, vol. 39, no. 3, pp. 672–676, May 2003.

[11] A. Radun, "High-power density switched reluctance motor drive for aerospace applications," *IEEE Transactions on Industry Applications*, vol. 28, no. 1, pp. 113–119, Jan. 1992.

[12] K. Kiyota and A. Chiba, "Design of switched reluctance motor competitive to 60-kW IPMSM in third-generation hybrid electric vehicle," *IEEE Transactions on Industry Applications*, vol. 48, no. 6, pp. 2303–2309, Nov. 2012.

[13] K. Vijayalakshmi and K. N. Srinivas, "Reduction of torque ripple, vibration and noise in switched reluctance motors focusing on electric vehicle applications: a survey," *International Journal of Vehicle Noise and Vibration*, vol. 17, no. 1–2, pp. 51–81, 2021.

Karunakaran Vijayalakshmi obtained her B.Eng. in Electrical and Electronics Engineering in Rajalakshmi Engineering College, India, in 2009 and M.Eng. in Embedded System Technology from Anna University, Chennai, India, in 2012. Currently, she is working as an Assistant Professor in the Department of Electrical and Electronics Engineering in SRM Institute of Science and Technology, Ramapuram Campus, Chennai, India. She is also a research scholar under the supervision of Dr. Srinivas in the same department, focusing on the research of electric machines and controllers for the application of electric vehicles, with particular use of finite element analysis.

Kandadai Nagaratnam Srinivas obtained his Diploma in Electrical and Electronics Engineering from the Chenkalvarayan Polytechnic, Chennai, India, in 1985, AMIE from the I.E. India in Electrical Engineering branch in 1989, M.E. in Power Systems from the Annamalai University, India, in 1993 and Ph.D. in Electrical Engineering from the Anna university, India, in 2004. He is a recipient of IEEE Best paper awards in the IEEE International Conferences IECON 2000 which was held in Japan and IECON 2003 which was held in the USA. He has about 120 International Journal and International conference publications. He has authored three text books for engineering students on the fundamentals of Electrical and Electronics Engineering. He has executed two funded projects from TNSCST and has completed a project on 3D magnetic field sensor project for DRDO, an Indian government defence organisation. His interests are power system contingency analysis, unit commitment and economic dispatch, modelling of electric drives and finite element analysis based electromagnetic and mechanical characterization of electrical machines - individually and for electric vehicle applications. Currently he is employed as HOD/EEE in SRM IST, Ramapuram Campus, chennai-89.